JOURNAL OF GEOPHYSICAL RESEARCH, VOL. 112, D12S01, doi:10.1029/2006JD007676, 2007

Click Here for Full Article

Measurement of HO_2NO_2 in the free troposphere during the Intercontinental Chemical Transport Experiment–North America 2004

S. Kim,[1] L. G. Huey,[1] R. E. Stickel,[1] D. J. Tanner,[1] J. H. Crawford,[2] J. R. Olson,[2] G. Chen,[2] W. H. Brune,[3] X. Ren,[3] R. Lesher,[3] P. J. Wooldridge,[4] T. H. Bertram,[4] A. Perring,[4] R. C. Cohen,[4] B. L. Lefer,[5,6] R. E. Shetter,[5] M. Avery,[2] G. Diskin,[2] and I. Sokolik[1]

Received 20 June 2006; revised 20 October 2006; accepted 14 November 2006; published 10 February 2007.

[1] The first direct in situ measurements of HO_2NO_2 in the upper troposphere were performed from the NASA DC-8 during the Intercontinental Chemical Transport Experiment–North America 2004 with a chemical ionization mass spectrometer (CIMS). These measurements provide an independent diagnostic of HO_x chemistry in the free troposphere and complement direct observations of HO_x, because of the dual dependency of HO_2NO_2 on HO_x and NO_x. On average, the highest HO_2NO_2 mixing ratio of 76 pptv (median = 77 pptv, σ = 39 pptv) was observed at altitudes of 8–9 km. Simple steady state calculations of HO_2NO_2, constrained by measurements of HO_x, NO_x, and J values, are in good agreement (slope = 0.90, R^2 = 0.60, and z = 5.5–7.5 km) with measurements in the midtroposphere where thermal decomposition is the major loss process. Above 8 km the calculated steady state HO_2NO_2 is in poor agreement with observed values (R^2 = 0.20) and is typically larger by a factor of 2.4. Conversely, steady state calculations using model-derived HO_x show reasonable agreement with the observed HO_2NO_2 in both the midtroposphere (slope = 0.96, intercept = 7.0, and R^2 = 0.63) and upper troposphere (slope = 0.80, intercept = 32.2, and R^2 = 0.58). These results indicate that observed HO_2 and HO_2NO_2 are in poor agreement in the upper troposphere but that HO_2NO_2 levels are consistent with current photochemical theory.

Citation: Kim, S., et al. (2007), Measurement of HO_2NO_2 in the free troposphere during the Intercontinental Chemical Transport Experiment–North America 2004, *J. Geophys. Res.*, *112*, D12S01, doi:10.1029/2006JD007676.

1. Introduction

[2] Pernitric acid (HO_2NO_2) is formed in the atmosphere by an association reaction that couples the HO_x and NO_x families [*Niki et al.*, 1977]:

$$\text{(R1)} \qquad HO_2 + NO_2 + M \leftrightarrow HO_2NO_2 + M$$

The thermal decomposition of HO_2NO_2, R-1, is a strong function of temperature with the lifetime for this process varying from approximately 20 s in the boundary layer to 8 hours at 8 km. Consequently, at lower and mid latitudes HO_2NO_2 is only expected to build up to significant concentrations in the upper troposphere, whereas photolysis and reaction with OH are expected to be the dominant loss processes.

$$\text{(R2)} \qquad HO_2NO_2 + h\nu \rightarrow \text{Products}$$

$$\text{(R3)} \qquad OH + HO_2NO_2 \rightarrow H_2O + NO_2 + O_2$$

[3] The potential impact of HO_2NO_2 on upper tropospheric photochemistry (z = 8–12 km) has been discussed by several investigators [*Brune et al.*, 1999; *Wennberg et al.*, 1999; *Faloona et al.*, 2000; *Jaeglé et al.*, 2000]. In particular, *Jaeglé et al.* [2000] noted the importance of HO_2NO_2 as a sink for HO_x at intermediate levels of NO_x (100–500 pptv) via R3. However, these studies were unconstrained by observations of HO_2NO_2. The only previous direct measurements of HO_2NO_2 are in the South Pole boundary layer during Austral Summer 2000 and 2003 [*Slusher et al.*, 2002; *Sjostedt et al.*, 2004]. These results demonstrated that HO_2NO_2 was present in significant levels (on average 25 pptv in 2000; 42 pptv in 2003) and could be

[1]School of Earth and Atmospheric Sciences, Georgia Institute of Technology, Atlanta, Georgia, USA.
[2]NASA Langley Research Center, Hampton, Virginia, USA.
[3]Department of Meteorology, Pennsylvania State University, University Park, Pennsylvania, USA.
[4]Department of Chemistry and Department of Earth and Planetary Science, University of California, Berkeley, California, USA.
[5]National Center for Atmospheric Research, Boulder, Colorado, USA.
[6]Now at Department of Geosciences, University of Houston, Houston, Texas, USA.

Copyright 2007 by the American Geophysical Union.
0148-0227/07/2006JD007676$09.00

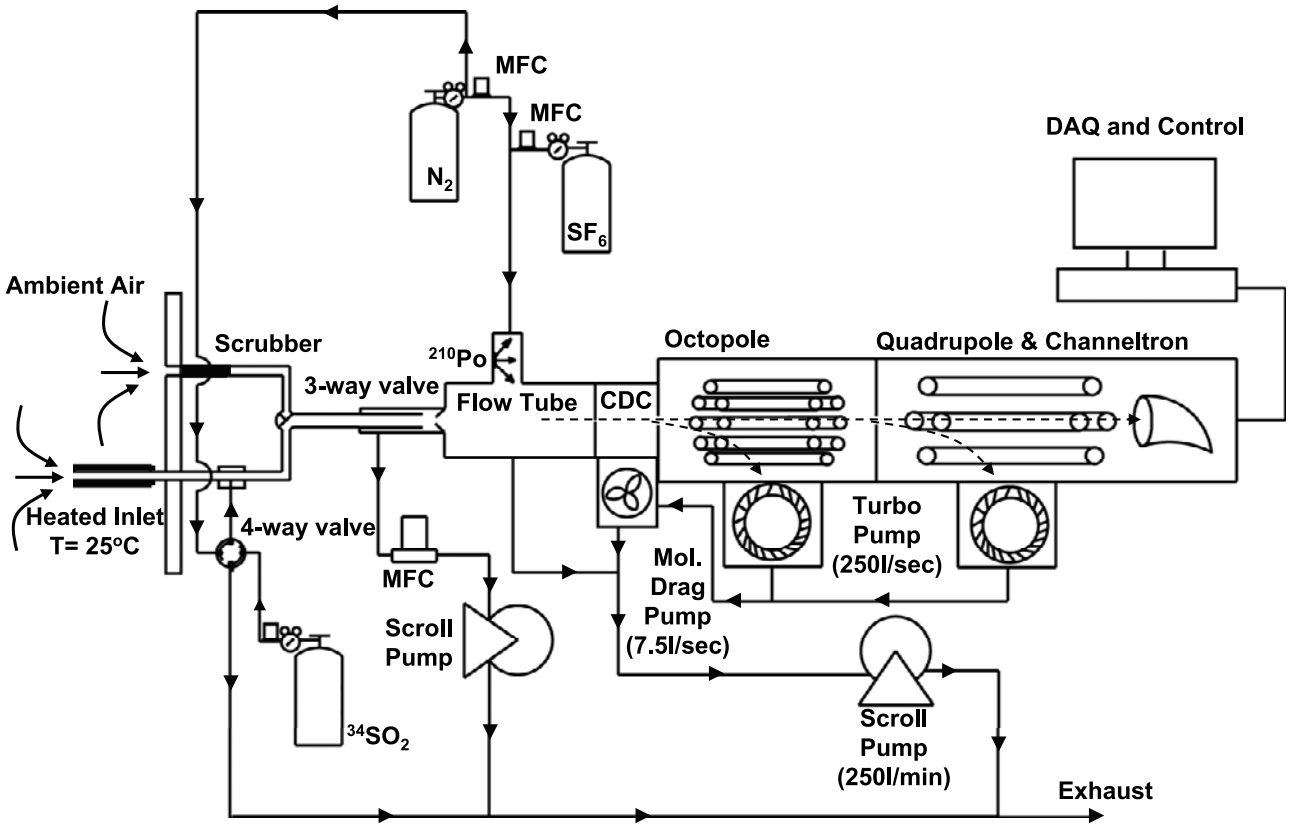

Figure 1. Diagram of CIMS system integrated on DC-8 for INTEX-NA 2004.

the dominant sink for HO_x via deposition to the snowpack and R3. The only in situ airborne HO_2NO_2 data were obtained during the TOPSE campaign from the NCAR C-130 at altitudes of 0 to 7 km. *Murphy et al.* [2003] derived levels of HO_2NO_2 + CH_3ONO_2 from their sum of peroxy nitrates channel (ΔPN) by subtracting independent measurements of peroxy acyl nitrates (PANs). They compared the derived HO_2NO_2 to photochemical calculations (with and without an overtone photolysis rate of 10^{-5} s^{-1}) and demonstrated the importance of the overtone photodissociation channel as a loss mechanism for HO_2NO_2 [*Roehl et al.*, 2002; *Wennberg et al.*, 1999]. Observations of pernitric acid by remote sensing have been reported but are confined to the stratosphere (20–40 km) [*Rinsland et al.*, 1996; *Sen et al.*, 1998].

[4] Here we present the first direct in situ observations of HO_2NO_2 in the free troposphere. These measurements were performed in the summer of 2004 with a chemical ionization mass spectrometer from the NASA DC-8 during the Intercontinental Chemical Transport Experiment–North America (INTEX-NA) field experiment. The INTEX-NA study sought to characterize and investigate the transport and transformation of both aerosol and gas-phase species over large spatial scales and altitude ranges. Flights were based out of California, Illinois, and New Hampshire. The sampling domain included much of the U.S., parts of Canada, and areas off the eastern and western coasts of North America. A detailed description of the DC-8 payload and the INTEX-NA campaign is presented by *Singh et al.* [2006]. In this work our understanding of the chemistry of HO_2NO_2 over the altitude range of 4–12 km is investigated by comparison of observations with highly constrained steady state calculations and photochemical models.

2. Methods

2.1. Instrumentation

[5] The instrument used to measure HO_2NO_2 and SO_2 from the NASA DC-8 during INTEX-NA is nearly identical to that described by *Slusher et al.* [2004]. The instrument comprises an inlet, a flow tube ion molecule reactor, a collisional dissociation chamber (CDC), an octopole ion guide and a quadrupole mass spectrometer as shown in Figure 1. SF_6^- ion chemistry is utilized to selectively ionize HO_2NO_2 and SO_2 (R4 and R5) in the CIMS [*Slusher et al.*, 2001; *Huey et al.*, 1995, 2004; *Huey*, 2006].

$$\text{(R4)} \qquad SF_6^- + HO_2NO_2 \rightarrow NO_4^-(HF) + SF_5$$

$$\text{(R5)} \qquad SF_6^- + SO_2 \rightarrow F_2SO_2^- + SF_4$$

Air was delivered to the CIMS through an all perfluoroalkoxy Teflon inlet (i.d. = 0.95 cm, length = 80 cm) maintained at a constant temperature of 298 K. A relatively low inlet temperature was utilized as the pernitric acid signal was found to diminish above 318 K because of thermal decomposition. A flow of more than 5 slpm was maintained in the inlet to minimize both the gas residence time ($t < 0.57$ s) and wall interaction. The sampled air was periodically scrubbed of both HO_2NO_2 and SO_2 with an activated carbon filter. The sensitivity of the instrument to SO_2 was

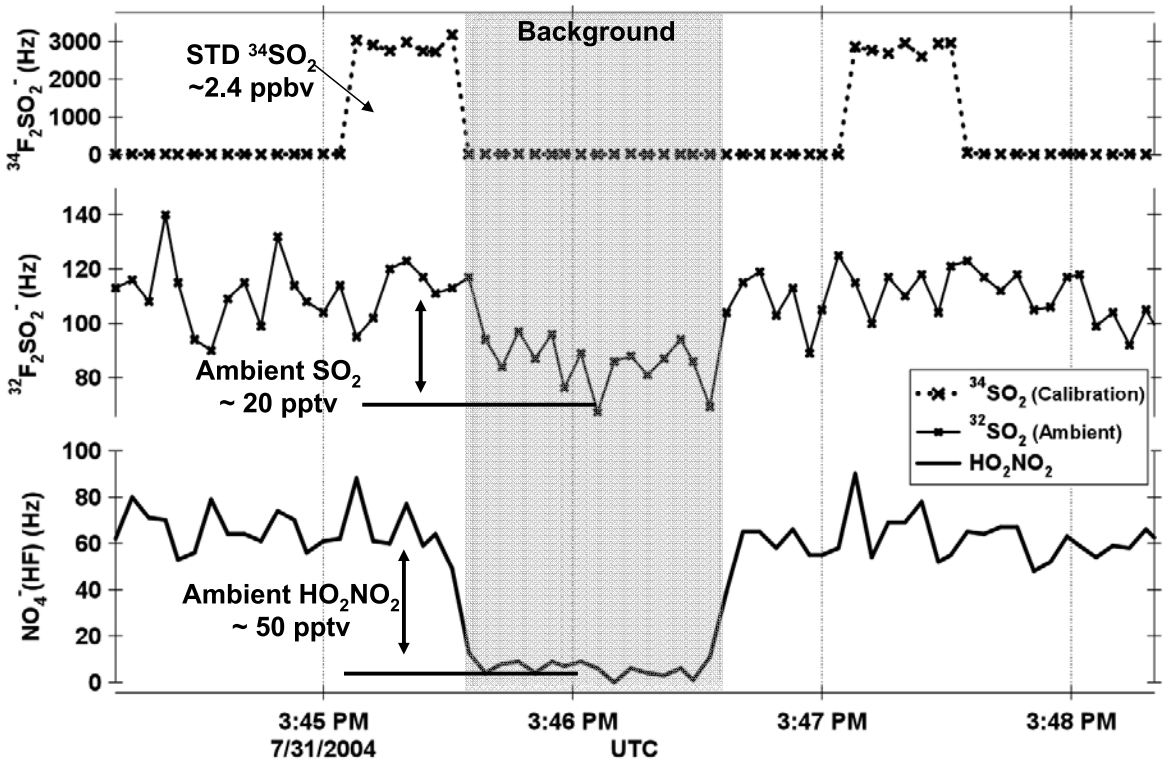

Figure 2. Raw ion signal obtained during flight. (top) The $^{34}SO_2$ signal illustrates the periodic calibration to the isotopically labeled standard. (middle) Ambient $^{32}SO_2$ signal. (bottom) Variation of ambient signal HO_2NO_2 signal. The shaded area is a background measurement period.

continuously monitored by the addition of isotopically labeled calibration gas (850 ppbv ± 9.2%) [e.g., *Bandy et al.*, 1993]. A typical example of the raw CIMS data is shown in Figure 2. The sensitivity of HO_2NO_2 relative to SO_2 was assessed post mission by a series of laboratory tests over the pressure and humidity conditions encountered on the DC-8. These tests demonstrated that the relative sensitivity of HO_2NO_2 to SO_2 was nearly identical to the ratio of the rate constants for reactions (R4) and (R5) [*Slusher et al.*, 2001]. This indicates that the sensitivity for both of these species is dominated by the ion molecule chemistry and that the continuous SO_2 calibration provides a good relative measure of the HO_2NO_2 sensitivity. The estimated uncertainty for HO_2NO_2 levels well above detection limit was typically less than 30% with a detection limit of less than 5 pptv for a 1-min integration at altitudes greater than 3 km.The methods used to obtain HO_x, NO_2, and J values during INTEX-NA have been described in detail elsewhere [*Avery et al.*, 2001; *Faloona et al.*, 2004; *Thornton et al.*, 2000; *Shetter and Müller* 1999].

2.2. Calculations

[6] HO_2NO_2 levels were estimated, assuming steady state, from the following equation.

$$[HO_2NO_2]_{ss} = \frac{k_1[HO_2][NO_2]}{J_2 + k_{-1} + k_3[OH]} \quad (1)$$

The rate constants for these calculations are taken from *Christensen et al.* [2004] for k_1, *Sander et al.* [2003] for k_{-1}, and *Jiménez et al.* [2004] for k_3. The NO_2 mixing ratios and the photolysis rate in the ultraviolet region were constrained by observations. Actinic fluxes in the near infrared were not measured during this campaign leaving the overtone photolysis rate unconstrained. For this reason, the overtone photolysis rate was estimated to be 10^{-5} s^{-1} [*Murphy et al.*, 2003; *Roehl et al.*, 2002; *Wennberg et al.*, 1999]. The uncertainty of $[HO_2NO_2]_{ss}$ calculated from the estimated error of each input parameter, excluding overtone photolysis, in equation (1) is ~68% at 8 km. The error in this calculation is dominated by the uncertainties in the HO_x measurement (~32%) and the rate constants k_{-1} and k_4 (~30%). The uncertainty does depend on altitude and ranges from 40 to 68%. Pernitric acid levels were calculated using both observed ($[HO_2NO_2]_{ss,obs}$) and model predicted ($[HO_2NO_2]_{ss,mod}$) levels of OH and HO_2. Model predicted HO_x levels were obtained from the NASA Langley photochemical box model which was highly constrained to observations of photolysis rates and the concentrations of long-lived species (e.g., NO_2, O_3, CO, etc.) [*Olson et al.*, 2004; *Crawford et al.*, 1999].

[7] Time-dependent model calculations were also performed to assess the deviation of HO_2NO_2 from steady state for typical upper tropospheric conditions where its lifetime is of the order of 5 hours (Figure 3). This method assumed an initial injection of NO_x into the upper troposphere and followed its temporal evolution and oxidation over the course of several days in 1-min time steps. Short-lived species such as radicals were predicted using the steady state assumption and the chemical scheme of

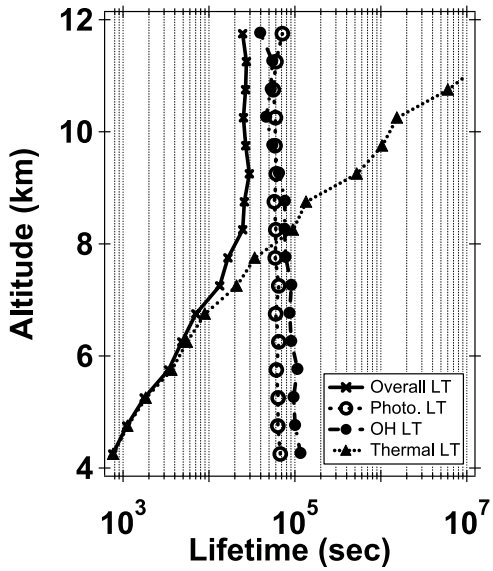

Figure 3. Vertical distribution of the total lifetime of HO_2NO_2 (x) and individual lifetimes with respect to thermal decomposition (triangles), photolysis (circles), and OH reaction (solid circles). The calculated values are based on INTEX-NA observations except for the overtone photolysis rate (10^{-5} s^{-1}).

Faloona et al. [2000]. Longer-lived species such as CO were held at median observed values. The chemical species and how they were treated in the model are listed in Table 1. All photolysis rates were calculated with the TUV 4.1 model (http://cprm.acd.ucar.edu/Models/TUV/) for conditions typical of INTEX-NA (e.g., latitude, time of day, and date), and rate constants were taken from the JPL evaluation version 14 [*Sander et al.*, 2003]. Calculated photolysis rates were found to be within 20% of observations during INTEX-NA.

3. Results and Analysis

[8] All reported data and analyses are based on a 1-min average merged data set (ftp://ftp-air.larc.nasa.gov/pub/INTEXA/DC8_AIRCRAFT/). The median observed HO_2NO_2 altitude profile for the INTEX-NA mission is presented in Figure 4, and the statistics of the vertical distribution are reported in Table 2. Median values of steady state calculations of HO_2NO_2 based on both observed and model predicted HO_x are also graphed in Figure 4. The observed HO_2NO_2 mixing ratio profile shows a maximum of ~76 pptv between 8 and 9 km. Pernitric acid mixing ratios decrease below this altitude as expected because of large thermal dissociation rates. Above 10 km levels decrease primarily because of a weakening of the source strength. The mean concentration of pernitric acid in the upper troposphere (8 ~ 12 km) was 67 ± 37 pptv (2467 data points, 1σ), which accounted for approximately 5% of the total reactive nitrogen (NO_y) budget and approximately 10% of the HO_x sink in this region as determined from the time-dependent modeling results described earlier (H. B. Singh et al., Reactive nitrogen distribution and budgets in the North American troposphere and lowermost stratosphere, submitted to *Journal of Geophysical Research,* 2006; X. Ren et al., unpublished manuscript, 2006).

[9] In the midtroposphere (4–8 km) both of the calculated profiles are in reasonable agreement with observations (Figure 4). This is more clearly illustrated in Figure 5 which presents scatterplots of the steady state calculations versus observations. The calculations based on observed HO_x (Figure 5a, R^2 = 0.60, slope = 0.90, intercept = 0.4 pptv) and on model predicted HO_x (Figure 5b, R^2 = 0.63, slope = 0.96 intercept = 7.0 pptv) are both well correlated to the observations. The median ratios for the calculations relative to the observations are 0.8 for observed HO_x and 1.1 for model predicted HO_x. This level of agreement is well within the 30% error bar of the HO_2NO_2 measurement alone. These results indicate that we have a reasonable understanding of the chemistry of HO_2NO_2 in this region, where thermal decomposition dominates the lifetime (Figure 3). Very similar results were also derived using k_{-1} from the recent work of *Gierczak et al.* [2005]. Correlations between calculations and observations were essentially identical with calculated values rising by a factor of 1.5. However, these results are still within the uncertainty of the analysis.

[10] In the upper troposphere (8–12 km) the agreement between the steady state calculations and observations is not as good as at lower altitudes. The HO_2NO_2 calculations based on model predicted HO_x are still highly correlated with the observations (Figure 6b, R^2 = 0.58, slope = 0.80, intercept = 32.2 pptv) but with a significant offset that yields a median ratio of calculated to observed of 1.3. Conversely, the correlation between HO_2NO_2 calculations based on observed HO_x and observations is significantly weaker (Figure 6a, R^2 = 0.20, slope = 1.38, intercept = 72.4 pptv) with a median ratio of calculated to observed of 2.4. These results indicate that our ability to predict HO_2NO_2 with simple steady state models at higher altitudes, where its lifetime is longer and controlled by photochemical processes (Figure 3), is not as good as at low altitudes. There is also a difference between upper tropospheric HO_x observations and predictions, especially around 10 km, with the pernitric acid observations more in accord with the photochemical model results.

Table 1. Summary of Chemical Species Treated in the Time-Dependent Model[a]

Category	Species
Constrained	O_3, CH_4, CO, CH_2O CH_3OOH, H_2O_2, $CH_3C(O)CH_3$, H_2O
Steady state	OH, HO_2, CHO, $O(^1D)$, CH_3O_2, $CH_3C(O)O_2$
Time dependent	NO, NO_2, HNO_3, HO_2NO_2, PAN, NO_3, N_2O_5

[a]Constrained species were held to median observed levels for the INTEX mission. The concentrations of the short-lived radicals (e.g., OH, HO_2, etc.) are calculated using the steady state assumption. The reactive nitrogen species (e.g., NO, HNO_3, etc.) are calculated in a time-dependent manner.

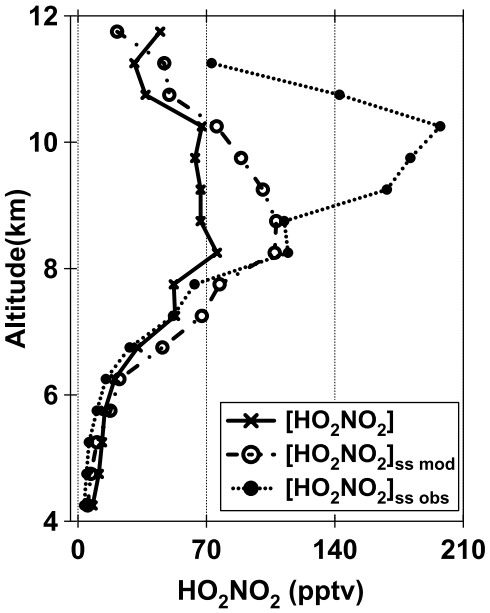

Figure 4. Vertical distribution of observed HO_2NO_2 (x) and predictions based on model predicted (open circles) and observed (solid circles) HO_x.

[11] At altitudes of 8–10 km the ratio of photochemical model predictions to observations (M/O) for OH and HO_2 are 1.8 and 1.0, respectively (X. Ren et al., unpublished manuscript, 2006). In the altitude range of 10–12 km the M/O ratio for OH and HO_2 are 1.5 and 0.5, respectively (X. Ren et al., unpublished manuscript, 2006). Consequently, there is a discrepancy between the measured and predicted HO_2 to OH ratio that increases with altitude. However, this difference is primarily due to the high levels of NO_x that also were observed to increase with altitude (T. H. Bertram et al., Direct measurements of the convective recycling of the upper troposphere, submitted to *Science,* 2006, hereinafter referred to as Bertram et al., submitted manuscript, 2006). The predicted ratio of $[HO_2]/[OH]$ decreases much more strongly as a function of NO_x than the observations (X. Ren et al., unpublished manuscript, 2006).

Table 2. Vertical Distribution of Observed HO_2NO_2 From 1-Min Average Data for INTEX-NA 2004

Altitude, km	Median, pptv	Average, pptv	1σ, pptv
4.25	8.0	12.3	15.9
4.75	11.4	15.8	20.7
5.25	13.4	31.3	62.7
5.75	15.6	20.5	15.5
6.25	20.4	25.6	18.4
6.75	32.2	38.9	24.0
7.25	53.7	59.2	32.4
7.75	51.9	61.5	39.3
8.25	78.2	77.5	39.6
8.75	66.8	75.1	39.9
9.25	67.8	75.8	41.4
9.75	62.6	65.0	32.5
10.25	63.0	66.1	29.7
10.75	38.7	44.1	25.2
11.25	34.1	41.0	23.8
11.75	46.0	46.8	10.7

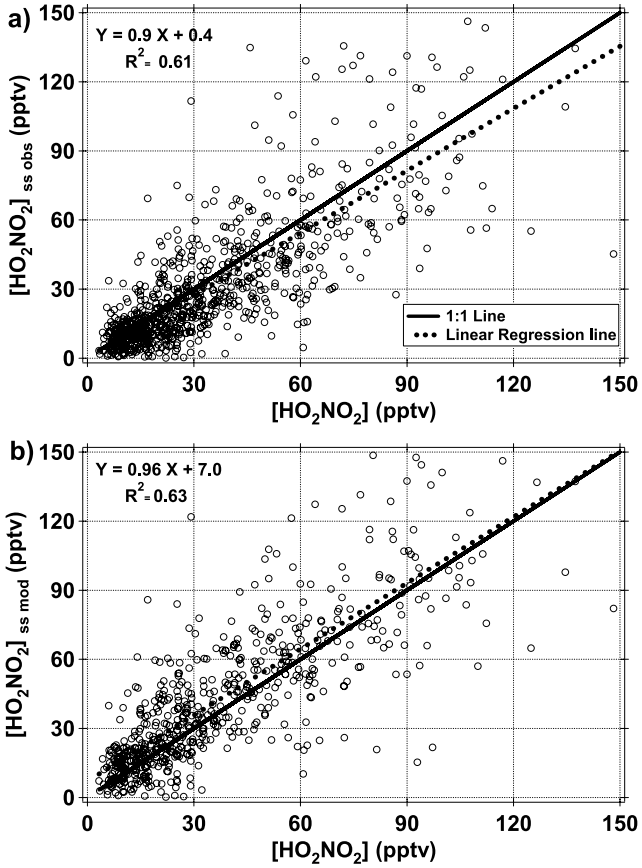

Figure 5. Scatterplots of midtroposphere (5.5–7.5 km) HO_2NO_2 steady state calculations versus observed HO_2NO_2. The calculations are based on (a) observed and (b) model HO_x.

[12] At higher altitudes where thermal decomposition of pernitric acid is negligible the ratio of HO_2NO_2 to NO_2 should have a strong dependence on the $[HO_2]/[OH]$ ratio. This is evident from equation (1) for those conditions where reaction with OH (R3) is the dominant loss. For the INTEX-NA mission the HO_2NO_2 loss due to OH dominates in the upper troposphere according to model predictions. However, if the model is incorrect the correlation between $[HO_2]/[OH]$ and $[HO_2NO_2]/[NO_2]$ should still be significant because of the dependence of OH levels on photolysis rates. Thus the observed $[HO_2NO_2]/[NO_2]$ ratio provides an independent check of the $[HO_2]/[OH]$ ratio. A strong correlation ($R^2 = 0.6$) is observed between model predicted $[HO_2]/[OH]$ (Figure 7b) and observed $[HO_2NO_2]/[NO_2]$; however, the correlation decreases significantly with observed HO_x (Figure 7a, $R^2 = 0.3$). The weaker correlation with the observations is primarily due to the insensitivity of the observed $[HO_2]/[OH]$ ratio to higher NO_x levels which corresponds to lower ratios of $[HO_2NO_2]/[NO_2]$. Consequently, the observed HO_2NO_2 levels are more consistent with the predicted $[HO_2]/[OH]$ ratio.

[13] Finally, the INTEX-NA data set allows the investigation of the impact of high levels of ozone on the CIMS system. A potential problem with the SF_6^- CIMS system for measurement of HO_2NO_2 is a positive interference due to high ozone levels [*Slusher et al.*, 2001]. This interference

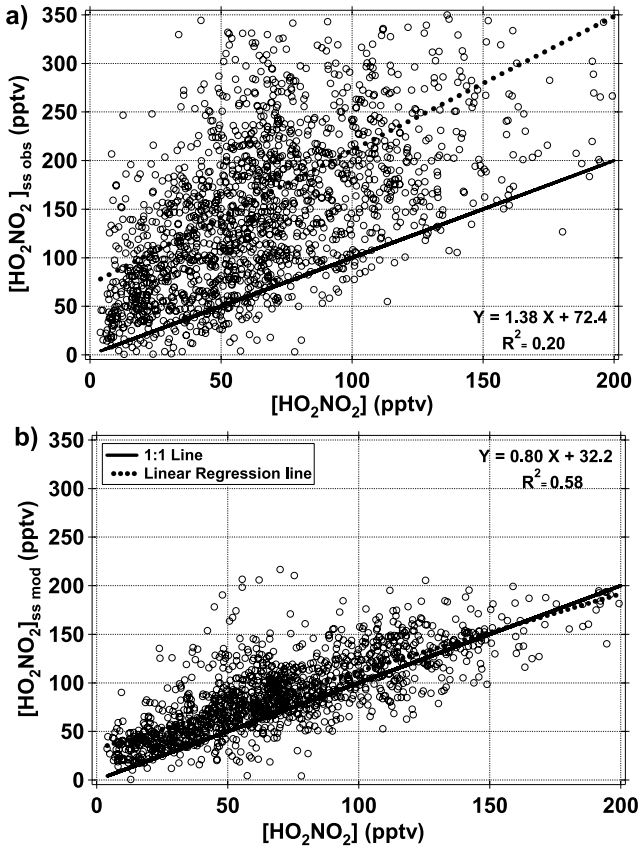

Figure 6. Scatterplots of upper troposphere (8–12 km) HO_2NO_2 steady state calculations versus observed HO_2NO_2. The calculations are based on (a) observed and (b) model HO_x.

has been characterized in the laboratory and was found to be unimportant at levels of ozone up to several hundred ppbv [*Slusher et al.*, 2001] but this has not been confirmed by field observations. The potential effect was investigated by examining the relationship of observed HO_2NO_2 with O_3. Figure 8 plots observed HO_2NO_2 versus O_3 in the altitude range 8.5–9.5 km (i.e., highest HO_2NO_2) for both periods when the air was primarily of tropospheric (O_3 < 150 ppbv, H_2O > 120 ppmv) and stratospheric origin (O_3 > 200 ppbv, H_2O < 100 ppmv). There is a moderate correlation (R^2 = 0.33) between pernitric acid and ozone at lower ozone levels for the tropospheric air masses. At the higher ozone levels in the stratospherically influenced air masses there is essentially no correlation. This indicates that O_3 at levels of up to 250 ppbv are not a significant interference to the HO_2NO_2 measurement. The correlation between ozone and HO_2NO_2 in the tropospheric air masses is likely due to ozone production via the reaction of HO_2 with NO which is closely related to pernitric acid formation (R1). This suggests that HO_2NO_2 in this altitude range may be a good marker for recent ozone production.

4. Discussion

[14] Measurements of HO_x, NO_x, and HO_2NO_2 were consistent at altitudes below 7.5 km where thermal decomposition dominates the loss of pernitric acid. The thermal decomposition rates derived from *Sander et al.* [2003] and *Gierczak et al.* [2005] are both in reasonable agreement with the lower-altitude observations. These results indicate that the uncertainty in the HO_2NO_2 lifetime due to the thermal decomposition rate, k_{-1}, is less than a factor of two at temperatures greater than 250 K.

[15] Above 8 km the observations of HO_x and HO_2NO_2 are less compatible with our understanding of photochemistry. The results indicate that the formation rate of HO_2NO_2 is overestimated or the loss rates are underestimated. Alternatively these results may suggest that the steady state calculations are problematic in this altitude range and the agreement between the model HO_x calculations and observed HO_2NO_2 is fortuitous. There is strong evidence that the rate constant (k_1) for the formation of HO_2NO_2 is accurately known. The rate constant has recently been measured by *Christensen et al.* [2004] and found to be within 15% of the JPL recommendation [*Sander et al.*, 2003], based on several previous studies, over a wide range of temperature and pressure. There has been speculation that the reaction of HO_2 with NO_2 could produce other products such as HONO, but this has been shown to be unimportant by *Tyndall et al.* [1995]. The rate constant, k_3, for the reaction of HO_2NO_2 with OH also appears to be known to better than 50% over a wide temperature range (218–335 K) [*Jiménez et al.*, 2004; *Smith et al.*, 1984]. This uncertainty is too little to bring the observed HO_x and HO_2NO_2 at

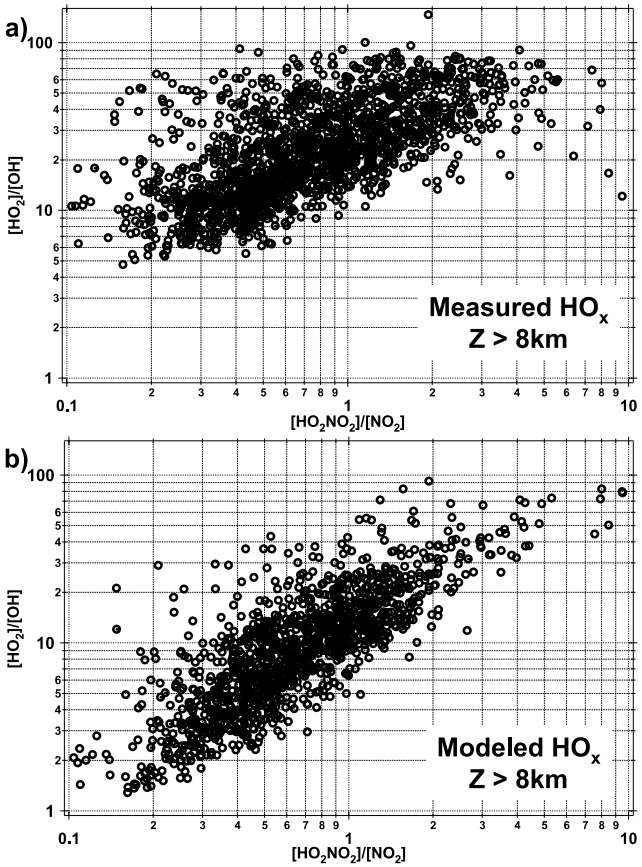

Figure 7. Correlation plot between $[HO_2NO_2]/[NO_2]$ and $[HO_2]/[OH]$ (a) from observed HO_x and (b) from model predicted HO_x.

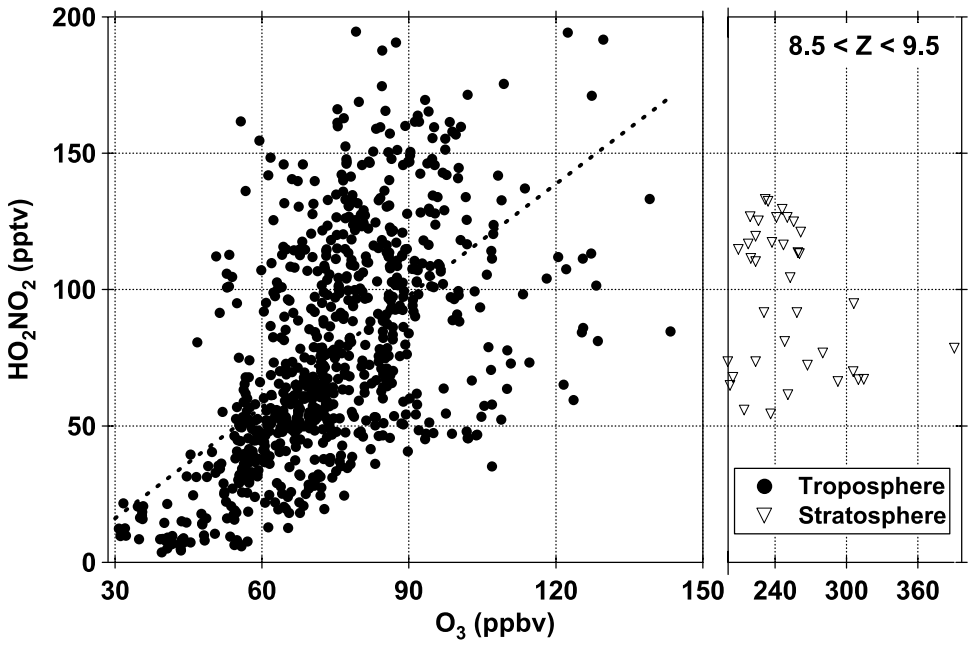

Figure 8. Scatterplot of HO_2NO_2 and O_3 in the altitude range of 8.5 to 9.5 km. Solid circles represent air primarily of tropospheric origin, and open triangles represent air with significant stratospheric influence. Note the horizontal axis has a change in scale at 150 ppbv of ozone.

higher altitudes into agreement. For these reasons, we have investigated other potential loss processes, reassessed our estimate of overtone photolysis rates, and performed time-dependent photochemical calculations to assess the magnitude of the deviation from steady state.

[16] Pernitric acid could be lost by heterogeneous loss or uptake in the upper troposphere on either background sulfate aerosol or cirrus clouds [*Evans et al.*, 2003]. However, we found no evidence for a relationship between aerosol surface area and HO_2NO_2 levels indicating that reaction on sulfate aerosol are not an important loss process. Evaluating the impact of cirrus clouds on pernitric acid levels is more problematic because of their relatively short lifetime (~1 hour). There were a few flight legs during the campaign in which the DC-8 sampled in cirrus clouds as evidenced by detection of large particles (>20 μm dia.). There was no obvious diminishment of pernitric acid in these air masses, but these data are limited and do not allow for a robust conclusion. For this reason, we think cirrus cloud processing of HO_2NO_2 is still an open question especially since pernitric acid has been shown to efficiently stick to ice at low temperatures [*Li et al.*, 1996].

[17] Overtone photolysis rates of HO_2NO_2 were estimated by calculating actinic fluxes using the SBDART (Santa Barbara DISORT Atmospheric Radiative Transfer) model [*Ricchiazzi et al.*, 1998] and cross sections and quantum yields from *Roehl et al.* [2002]. Calculations of both direct and diffuse fluxes were performed for typical INTEX conditions as listed in Table 3. Note that sand was chosen as the surface to maximize the infrared albedo. A total photolysis rate of 8.0×10^{-6} s^{-1} was calculated which compares favorably with the value of 8.3×10^{-6} s^{-1} derived by *Roehl et al.* [2002] from the direct flux at the top of the atmosphere. These calculations indicate the photolysis rate (10^{-5} s^{-1}) used in the steady state analysis is reasonable but is probably an upper limit. As the dominant overtone photolysis band, $2\nu_1$, for HO_2NO_2 overlaps a water transition [*Rothman et al.*, 2005] the upward flux in this spectral range over clouds, ocean, and snowpack will be attenuated because of a decreased albedo in the near-IR. It is also worth noting that only one measurement [*Roehl et al.*, 2002] of the quantum yield and cross section for the $2v_1$ band is available and should probably be confirmed.

[18] The error in the HO_2NO_2 calculations was investigated by using a time-dependent photochemical model to estimate the deviation from steady state. Figure 9 shows a temporal plot of HO_2NO_2 at 9 km, for typical INTEX-NA conditions (28 July, latitude ~40°N), calculated using steady state and time-dependent methods. The time-dependent results are for the second day after a fresh injection of NO_x into the upper atmosphere reflecting the relatively fresh air masses sampled during INTEX-NA (Bertram et al., submitted manuscript, 2006; H. E. Fuelberg et al., Meteorological conditions and anomalies during INTEX-NA, submitted to *Journal of Geophysical Research,* 2006; M. Porter et al., unpublished manuscript, 2006). However, the comparison of the time-dependent and steady state results was not found to depend strongly on the number of days after the NO_x injection. In fact, the steady state values were found to be within 50% of the time-dependent

Table 3. Parameters for Actinic Flux Calculations Using SBDART

Local Time	28 July, Local Noon
Latitude	38°N
Surface type	sand
Atmosphere profile	US 62
Boundary layer type	rural

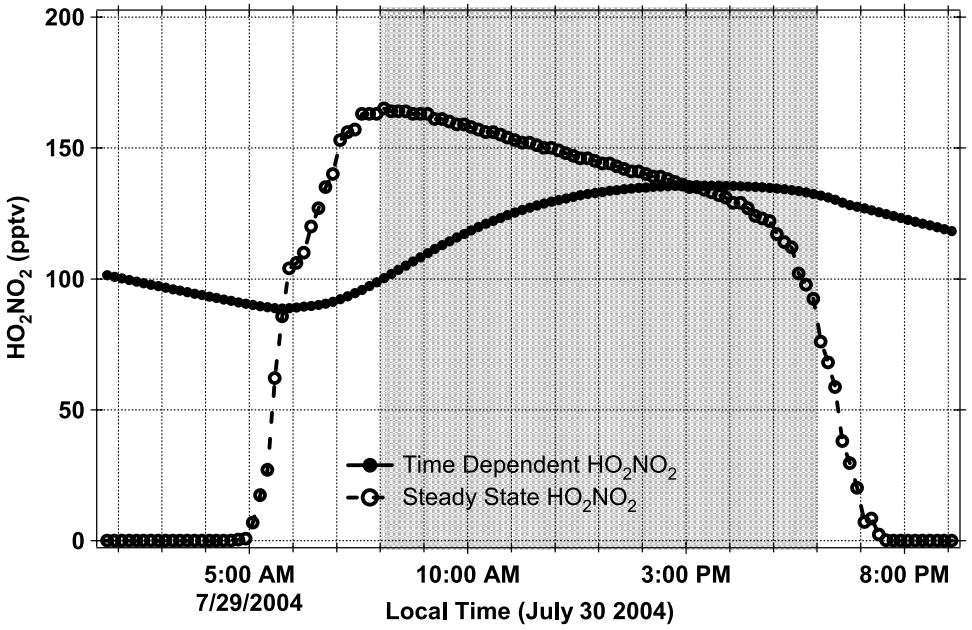

Figure 9. Temporal plot of HO_2NO_2 calculated using time-dependent (solid circle with solid line) and steady state HO_2NO_2 (open circle with dashed line) models. Shaded time zone is a typical flight time during INTEX-NA from 0800 to 1800 LT.

calculations within approximately 5 hours after a fresh injection of NO_x. The shaded area in Figure 9 is the typical flight time from 0800 to 1800 LT. The largest difference is in the morning where the steady state model overpredicts HO_2NO_2 by ~50%. The disagreement diminishes through the day until there is a slight underestimation by the steady state model in the late afternoon. These effects were observed to a small extent in the data as the ratio of model predictions to observations before noon was approximately 10% greater than in the afternoon. On average the steady state model overpredicts the time-dependent results by 12% during typical DC-8 flight times. At higher altitudes the disagreement between steady state and time-dependent calculations is lower as HO_2NO_2 does not undergo signifi-

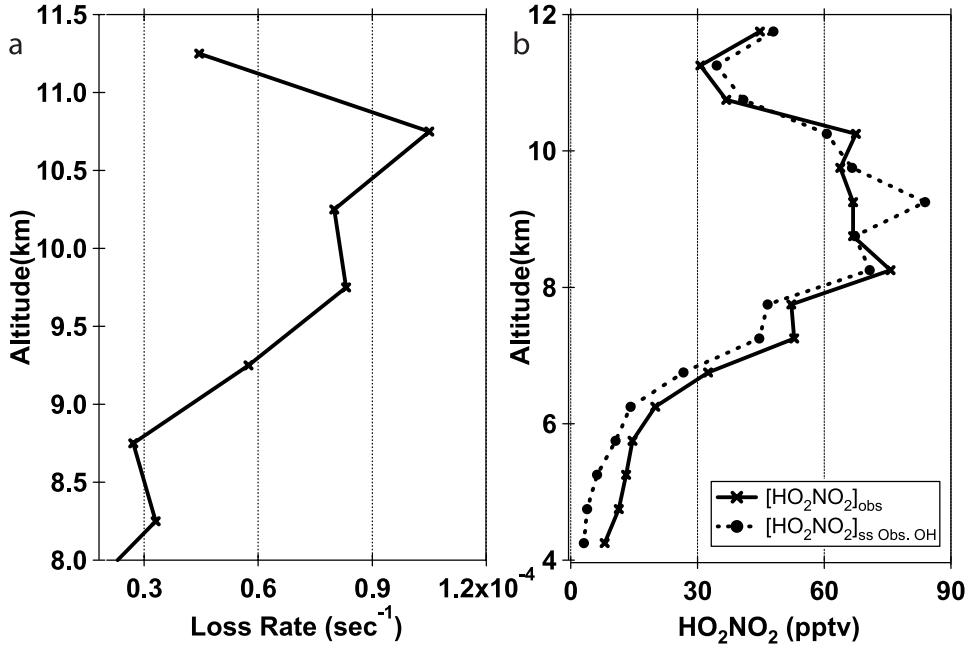

Figure 10. (a) Altitude profile of the first-order rate constant for the additional loss of HO_2NO_2 derived from measured HO_x. (b) Vertical profile of observed ($[HO_2NO_2]_{obs}$) and predicted ($[HO_2NO_2]_{ss\_Obs.\ OH}$). The predicted HO_2NO_2 is derived from a steady state analysis using observed OH levels and the model predicted ratio of $[HO_2]$ to [OH].

cant thermal decomposition through the night. Consequently, steady state methods seem to be valid for predicting HO_2NO_2 levels in the upper troposphere with less than a 50% inherent error bar.

[19] Clearly, the measured HO_2NO_2 and HO_x are not consistent with our current understanding of photochemistry in the upper troposphere. One possible explanation is that there are unidentified measurement errors in either or both the HO_x and HO_2NO_2 measurements. These potential errors must be greater at either high altitude or high NO_x levels, but at this point we are unaware of any mechanisms for these errors. Alternatively, a higher loss rate for pernitric acid would bring observations of HO_2NO_2 and HO_2 into better agreement. Figure 10a presents the vertical profile of the needed HO_2NO_2 first-order rate constant for the additional loss needed to bring observed HO_2NO_2 and HO_x into accord. This additional loss rate generally increases with altitude with a maximum near 11 km. The needed loss rate is of a large magnitude and is unlikely to be explained by any single mechanism. One potential mechanism that could account for some of the additional loss is photolysis via weak electronic transitions as discussed by *Mathews et al.* [2005]. Finally, we determined if the measured OH and the model predicted $[HO_2]/[OH]$ ratio are consistent with the observed HO_2NO_2. This was done with a steady state analysis using observed OH and HO_2 derived from the predicted HO_x ratio. The median altitude profile for this data is shown in Figure 10b and shows excellent agreement with the observed profile. These data demonstrate that the observed HO_2NO_2 are inconsistent with the observed HO_x ratio but not the observed OH levels.

5. Summary

[20] Our understanding of HO_2NO_2 in the free troposphere is examined with the first direct in situ observations from the NASA DC-8 during INTEX-NA 2004. Photochemical models and observed HO_x levels can explain the HO_2NO_2 in the midtroposphere (4.5–8 km) where thermal decomposition is dominant. In the upper troposphere (8–12 km) there is a significant discrepancy between model predicted and observed HO_x. There is also significant disagreement between steady state calculations of HO_2NO_2 that use measured HO_2 levels and observations of HO_2NO_2 in the upper troposphere. Conversely, pernitric acid levels are reasonably well predicted by steady state calculations using photochemical model predicted HO_2 levels. Time-dependent modeling of HO_2NO_2 levels indicates that treating pernitric acid as in steady state is valid in the upper troposphere. The discrepancy between the observed HO_2 and HO_2NO_2 levels would be diminished if there is an unidentified loss process for HO_2NO_2 whose magnitude increases with altitude. This suggests that further investigation of potential HO_2NO_2 loss process may be needed.

[21] **Acknowledgments.** The authors gratefully acknowledge the financial support of NASA through contract NNG04GB62G and thank the DC-8 crew and support team. We also thank Paul Ricchiazzi of U.C. Santa Barbara for valuable advice on using SBDART.

References

Avery, M. A., D. J. Westberg, H. E. Fuelberg, R. E. Newell, B. E. Anderson, S. A. Vay, G. W. Sachse, and D. R. Blake (2001), Chemical transport across the ITCZ in the central Pacific during an El Niño-Southern Oscillation cold phase event in March–April 1999, *J. Geophys. Res.*, *106*(D23), 32,539–32,554.

Bandy, A. R., D. C. Thornton, and A. R. Driedger III (1993), Airborne measurements of sulfur dioxide, dimethyl sulfide, carbon disulfide, and carbonyl sulfide by isotope dilution gas chromatography/mass spectrometry, *J. Geophys. Res.*, *98*(D12), 23,432–23,433.

Brune, W. H., et al. (1999), OH and HO_2 chemistry in the North Atlantic free troposphere, *Geophys. Res. Lett.*, *25*, 1701–1704.

Christensen, L. E., M. Okumura, S. P. Sander, R. R. Friedl, C. E. Miller, and J. J. Sloan (2004), Measurements of the rate constant of $HO_2 + NO_2 + N_2 \rightarrow HO_2NO_2 + N_2$ using near-infrared wavelength-modulation spectroscopy and UV-visible absorption spectroscopy, *J. Phys. Chem. A*, *108*, 80–91.

Crawford, J., et al. (1999), Assessment of upper tropospheric HO_x sources over the tropical Pacific based on NASA GTE/PEM data: Net effect on HO_x and other photochemical parameters, *J. Geophys. Res.*, *104*(D13), 16,255–16,273.

Evans, M. J., et al. (2003), Coupled evolution of BrO_x-ClO_x-HO_x-NO_x chemistry during bromine-catalyzed ozone depletion events in the arctic boundary layer, *J. Geophys. Res.*, *108*(D4), 8368, doi:10.1029/2002JD002732.

Faloona, I., et al. (2000), Observations of HO_x and its relationship with NOx in the upper troposphere during SONEX, *J. Geophys. Res.*, *105*(D3), 3771–3783.

Faloona, I. C., et al. (2004), A laser-induced fluorescence instrument for detecting tropospheric OH and HO_2: Characteristics and calibration, *J. Atmos. Chem.*, *47*, 139–167.

Gierczak, T., E. Jiménez, V. Riffault, J. B. Burkholder, and A. R. Ravishankara (2005), Thermal decomposition of HO_2NO_2 (peroxynitric acid, PNA): Rate coefficient and determination of the enthalpy of formation, *J. Phys. Chem. A*, *109*, 586–596.

Huey, L. G. (2006), Measurement of trace atmospheric species by chemical ionization mass spectrometry: Speciation of reactive nitrogen and future directions, *Mass Spectrom. Rev*, in press.

Huey, L. G., D. R. Hanson, and C. J. Howard (1995), Reactions of SF_6^- and I^- with atmospheric trace gases, *J. Phys. Chem.*, *99*, 5001–5008.

Huey, L. G., et al. (2004), CIMS measurements of HNO_3 and SO_2 at South Pole during ISCAT 2000, *Atmos. Environ.*, *38*, 5411–5421.

Jaeglé, L., et al. (2000), Photochemistry of HO_x in the upper troposphere at northern mid-latitude, *J. Geophys. Res.*, *105*, 3877–3892.

Jiménez, E., T. Gierczak, H. Stark, J. B. Burkholder, and A. R. Ravishankara (2004), Reaction of OH with HO_2NO_2 (pernitric acid): rate coefficient between 218 and 225 K and product yields at 298K, *J. Phys. Chem. A*, *108*, 1139–1149.

Li, Z., R. R. Friedl, S. B. Moore, and S. P. Sander (1996), Interaction of peroxynitric acid with solid H_2O ice, *J. Geophys. Res.*, *101*(D3), 6759–6802.

Mathews, J., A. Sinha, and J. S. Francisco (2005), The importance of weak absorption features in promoting tropospheric radical production, *Proc. Natl. Acad. Sci. U.S.A.*, *102*(21), 7449–7452.

Murphy, J. G., J. A. Thornton, P. J. Wooldridge, D. A. Day, R. S. Rosen, C. Cantrell, R. Shetter, B. Lefer, and R. C. Cohen (2003), Measurements of the sum of HO_2NO_2 and $CH_3O_2NO_2$ in the remote troposphere, *Atmos. Chem. Phys. Disc.*, *3*(6), 5689–5710.

Niki, H., P. D. Marker, C. M. Savage, and L. P. Breitenbach (1977), Fourier transform IR spectroscopy observation of pernitric acid formed via $HOO + NO_2 \rightarrow HOONO_2$, *Chem. Phys. Lett.*, *45*(3), 564–566.

Olson, J. R., et al. (2004), Testing fast photochemical theory during TRACE-P based on measurements of OH, HO_2 and CH_2O, *J. Geophys. Res.*, *109*, D15S10, doi:10.1029/2003JD004278.

Ricchiazzi, P., S. Yang, C. Gautier, and D. Sowle (1998), SBDART: A research and teaching software tool for plane-parallel radiative transfer in the Earth's atmosphere, *Bull. Am. Meteorol. Soc.*, *79*(10), 2101–2114.

Rinsland, C. P., et al. (1996), ATMOS/ATLAS-3 measurements of stratospheric chlorine and reactive nitrogen partitioning inside and outside the November 1994 Antarctic vortex, *Geophys. Res. Lett.*, *23*(17), 2365–2368.

Roehl, C. M., S. A. Nizkorodov, H. Zhang, G. Blake, and P. O. Wennberg (2002), Photodissociation of peroxynitric acid in the Near-IR, *J. Phys. Chem.*, *106*, 3766–3772.

Rothman, L. S., et al. (2005), The HITRAN 2004 molecular spectroscopic database, *J. Quant. Spectrosc. Radiat. Transfer*, *96*, 139–204.

Sander, S. P., A. R. Ravishankara, D. M. Golden, C. E. Kolb, M. J. Kurylo, R. E. Huie, V. L. Orkin, M. J. Molina, G. K. Moortgat, and B. J. Finlayson-Pitts (2003), Chemical kinetics and photochemical data for use in atmospheric studies, *JPL Publ. 02-25*, NASA Jet Propul. Lab., Pasadena, Calif.

Sen, B., G. C. Toon, G. B. Osterman, J.-F. Blavier, J. J. Margitan, R. J. Salawitch, and G. K. Yue (1998), Measurements of reactive nitrogen in the stratosphere, *J. Geophys. Res.*, *103*(D3), 3571–3585.

Shetter, R. E., and M. Müller (1999), Photolysis frequency measurements using actinic flux spectroradiometry during the PEM-Tropics mission: Instrumentation description and some result, *J. Geophys. Res.*, *104*(D5), 5647–5661.

Singh, H. B., W. Brune, J. Crawford, and D. Jacob (2006), Overview of the summer 2004 Intercontinental Chemical Transport Experiment–North America (INTEX-A), *J. Geophys. Res.*, *111*, D24S01, doi:10.1029/2006JD007905.

Sjostedt, S. J., D. J. Tanner, J. E. Dibb, M. Buhr, M. Warshawsky, D. Davis, G. Chen, R. L. Mauldin, F. L. Eisele, R. Arimoto, and L. G. Huey (2004), Measurements HO_2NO_2 and HNO_3 at South Pole during ANTCI 2003, *Eos Trans. AGU*, *85*(47), Fall Meet. Suppl., Abstract A24A-02.

Slusher, D. L., S. J. Pitteri, B. J. Haman, D. J. Tanner, and L. G. Huey (2001), A chemical ionization technique for measurement of pernitric acid in the upper troposphere and the polar boundary layer, *Geophys. Res. Lett.*, *28*, 3875–3878.

Slusher, D. L., et al. (2002), Measurements of pernitric acid at the south pole during ISCAT 2000, *Geophys. Res. Lett.*, *29*(21), 2011, doi:10.1029/2002GL015703.

Slusher, D. L., L. G. Huey, D. J. Tanner, F. Flocke, and J. M. Roberts (2004), A thermal dissociation-chemical ionization mass spectrometry (TD-CIMS) technique for the simultaneous measurement of peroxyacyl nitrates and dinitrogen pentaoxide, *J. Geophys. Res.*, *109*, D19315, doi:10.1029/2004JD004670.

Smith, C. A., L. T. Molina, J. J. Lamb, and M. J. Molina (1984), Kinetics of the reaction of OH with pernitric and nitric-acids, *Int. J. Chem. Kinet.*, *16*(1), 41–55.

Thornton, J. A., P. J. Wooldridge, and R. C. Cohen (2000), Atmospheric NO_2: In situ laser-induced fluorescence detection at parts per trillion mixing ratios, *Anal. Chem.*, *72*(3), 528–539.

Tyndall, G. S., J. J. Orlando, and J. G. Calvert (1995), Upper limit for the rate coefficient for the reaction $HO_2 + NO_2 \rightarrow HONO + O_2$, *Environ. Sci. Technol.*, *29*(1), 202–206.

Wennberg, P. O., et al. (1999), Twilight observations suggest unknown sources of HOx, *Geophys. Res. Lett.*, *26*, 1373–1376.

M. Avery, G. Chen, J. H. Crawford, G. Diskin, and J. R. Olson, NASA Langley Research Center, Hampton, VA 23681, USA.

T. H. Bertram, R. C. Cohen, A. Perring, and P. J. Wooldridge, Department of Chemistry and Department of Earth and Planetary Science, University of California, Berkeley, CA 94720, USA.

W. H. Brune, R. Lesher, and X. Ren, Department of Meteorology, Pennsylvania State University, University Park, PA 16802, USA.

L. G. Huey, S. Kim, I. Sokolik, R. E. Stickel, and D. J. Tanner, School of Earth and Atmospheric Sciences, Georgia Institute of Technology, Atlanta, GA 30332, USA. (greg.huey@eas.gatech.edu)

B. L. Lefer, Department of Geosciences, University of Houston, Houston, TX 77204, USA.

R. E. Shetter, National Center for Atmospheric Research, Boulder, CO 80305, USA.